Magnetic dipolarizations inside geosynchronous orbit with tailward ions flow

Xiaoying Sun[1,2], Weining William Liu [1], Suping Duan[1]

[1] State Key Laboratory of Space Weather, National Space Science Center (NSSC),Chinese Academy of Sciences (CAS), Beijing, 100190, China
[2]University of Chinese Academy of Sciences, Beijing, 100049, China

Correspondence to: W .W. Liu (wliu@nssc.ac.cn), Suping Duan (spduan@nssc.ac.cn)

Abstract. Electromagnetic field and plasma data from the Time History of Events and Macroscale Interactions duringSubstorms (THEMIS) near-Earth probes are used to investigate magnetic dipolarizations inside geosynchronous orbit on 27 August 2014 during an intense substorm with AE_{max} ~ 1000nT. THEMIS-D (TH-D) was located inside geosynchronous orbit around midnight in the interval from 09:25 UT to 09:55 UT. During this period two distinct magnetic dipolarizations with tailward ions flow are observed by TH-D. The first one is displayed by magnetic elevation angle increase from 15 degree to 25 degree around 09:30:40UT. The tailward perpendicular velocity is $V_{\perp x}$ ~ -50km/s. The second one is presented by the elevation angle increase from 25 degree to 45 degree around 09:36 UT. And the tailward perpendicular velocity is $V_{\perp x}$ ~ -70 km/s. These two significant dipolarizations are accompanied with the sharp increase in the energy flux of energetic electron inside geosynchronous. After 5 min expanding of near-Earth plasma sheet (NEPS), THEMIS-E (TH-E) located outside geosynchronous orbit also detects this tailward expanding plasma sheet with ion flow -150 km/s. The dipolarization propagates tailward with speed -47 km/s, along 2.2 R_E distance in the X direction between TH-D and TH-E within 5 min. These dipolarizations with tailward ions flow observed inside geosynchronous orbit indicate new energy transfer path in the inner magnetosphere during substorms.

Keywords: Magnetic dipolarization, tailward ions flow, near-Earth plasma sheet, intense substorm

Introduction

Magnetic dipolarization can be observed at or inside geosynchronous orbit during intense substorms with high AE index (AE > 500 nT) [e.g., Dai et al., 2015; Nagai, 1982; Nosé et al., 2014; Ohtani et al., 2018]. Dipolarizations are marked by the magnetic elevation angle increase with the decrease in the radial components of B_x and B_y, and the increase in the B_z component [Liu and Liang, 2009; Duan et al., 2011; Dai et al., 2014, 2015]. Ohtani et al. [2018] presented the statistics characteristics of magnetic dipolarizations inside geosynchronous orbit. They reported that the dipolarization region expanded in the azimuthal direction with speed 60 km/s at 5.5 R_E. Using multiple satellites conjunction observations at or

inside geosynchronous orbit, Dai et al. [2015] reported thatthe large dipolarization electric field was associated with substorm injection of MeV electrons into the inner magnetosphere (r < 6.6 R_E).

Magnetic dipolarizations are accompanied with complex ions bulk flow in the near-Earth plasma sheet (NEPS) [e.g., Duan et al., 2008; Liang et al., 2009]. Especially, it is more complex in the inner edge of ~~NESP~~ NEPS. Usually, the substorm-associated dipolarizations in the NEPS are accompanied with earthward ions bulk flow [e.g., Angelopoulos et al., 1992; Baumjohann et al., 1999; Duan et al., 2011; Liang et al., ~~2008~~ 2009; Liu et al., 2008; Nakamura et al., 2009; Shiokawa et al., 1998]. According conjunction observations of THEMIS multiple probes in the NEPS, Duan et al. [2011] pointed out that the dipolarization at inner edge of the near-Earth plasma sheet had no one-to-one relationship with the earthward ions bulk flow. Lui et al. [1999] pointed out that dipolarization at X~$10R_E$ was detected with tailward flow. Inside geosynchronous orbit, magnetic dipolarizations were detected with earthward ions bulk flow [Dai et al., 2015].

Near-Earth Dipolarizations with low frequency waves are detected with thermal ions and electron energization [e.g., Dai et al., 2015; Liang et al., ~~2008,~~ 2009; Nosé et al., 2014; Ohtani et al., 2018]. These energetic particles are main source of inner magnetosphere during substorms and storms. Nosé et al. [2014] proposed that the dipolarizations associated with low frequency fluctuations were observed in the inner magnetosphere during the storm main phase. These low frequency electromagnetic waves can accelerate O^+ ions in the perpendicular direction. The low frequency waves can accelerate particles crossing the magnetic field with large perpendicular electric field [e.g., Dai et al., 2014, 2015; Duan et al., 2016; Nosé et al., 2014]. Usually, Dipolarization associated dispersionless energetic particle injections is accompanied with earthward ions bulk flow in the NEPS [Dai et al., 2015]. But few reports show that dipolarizations with the sharply increase in the energy flux of energetic particles associated with tailward ions flow at or inside geosynchronous orbit.

The ballooning mode occurred in the near-Earth plasma sheet are associated with tailward expansion of plasma sheet during substorms [Liu, 1997; Liu et al., 2008; Liu and Liang, 2009; Liang et al., 2009; Saito et al., 2008]. Liu et al. [2008] pointed out that the ballooning mode could excite a quasi-electrostatic field a few minutes before local current disruption and that the perturbations associated with ballooning instability propagated downtail.

In this paper we present ~~a~~ dipolarizations with tailward ions flow inside geosynchronous orbit during an intense substorm expansion phase. The observations in detail of an intense substorm on 27 August 2014 by TH-D and TH-E are presented in section 2. Discussions and conclusions of our observation results are displayed in the last section.

Observations of an intense substorm on 27 August 2014

The OMNI data of the solar wind, interplanetary magnetic field (IMF) and geomagnetic field index Dst and AE during a storm on August 27, 2014 are presented in Figure 1. The minimum value of ~~Dst~~ SYM-H index is about ~~-80~~ -90 nT, as shown in Figure ~~1e~~ 1f, imply that a moderate storm take placed. During the main phase of this moderate storm, there is an intense substorm with the AE maximum value ~~1273~~ 700 nT around 10:10 UT. The beginning time of this intense substorm expansion phase is around 09:31 UT with decrease in the AL index. A significant substorm enhancement occur around 09:48 UT with sharply decrease in the AL index and increase in the AE index.

During this intense substorm, THEMIS probes [Angelopoulos, 2008], such as TH-D and TH-E are both located in the near-Earth magnetotail. Figure 2 displays the orbits of TH-D and TH-E from 09:20 to 10:00 UT in the SM coordinate system. At 09:30 UT, locations of these two spacecraft in SM coordinates, are (~~-6.01~~ -6.10, -0.06, ~~1.12~~ 0.43) R_E for TH-D, (~~-8.10~~ -8.26, -2.28, ~~1.92~~ 0.99) R_E for TH-E, respectively. TH-D orbit plot presents that it is located inside geosynchronous orbit at the beginning time of this intense substorm expansion phase. On the other hand, TH-E is located outside geosynchronous orbit. These two spacecraft present good conjunction observations during this intense substorm expansion phase. The instruments adopted in our investigations are thefluxgate magnetometer (FGM) [Auster et al., 2008], the electrostatic analyzer (ESA) [McFadden et al., 2008], the electric field instrument (EFI) [Bonnell et al., 2008] and the solid state telescope (SST) on board the THEMIS probes.

Figure 3 shows the plasma parameters and the electromagnetic field detected by TH-D mostly inside geosynchronous orbit at about midnight section. The solar magnetic (SM) coordinate system is adopted. From top to bottom, panels are the total magnetic field value, B_t and the B_x component, the B_y and B_z components, the magnetic field elevation angle defined by $\theta = \tan^{-1}(B_z/({B_x}^2 + {B_y}^2)^{1/2})$, the ion and electron density, temperature, the plasma beta value β, $\beta = 2\mu_0 nT/B^2$, which determines the location of the satellite [Miyashita et al., 2000], three components of ions bulk flow velocity parallel (black line) and perpendicular (red line) to the magnetic field, V_x, V_y and V_z, three components of the electric field, the E_x (red), the E_y (black) and the E_z (blue), there components of convection electric field from $\mathbf{V}\times\mathbf{B}$, the E_{cx} (red), the E_{cy} (black) and the E_{cz}(blue), respectively. Figure 3 displays the distinct fluctuations of the magnetic field and plasma density and velocity around 09:30 UT and 09:36 UT, respectively. The magnetic elevation angle has two step clear enhancements as displayed in Figure 3c. The first increase in elevation angle is from about 15 degree to 25 degree during the interval from 09:30:34 UT to 09:30:54 UT, which are marked by the left two vertical dashed lines in Figure 3. The total magnetic field value and the B_x component both decrease. The B_z component increase weakly from about 35 nT to 45 nT. The B_y component has obvious fluctuations around 0 nT. These magnetic signatures indicate a magnetic dipolarization take places inside geosynchronous orbit around (-6.10, -0.06, 0.43) R_E. During this weak magnetic field dipolarization, the plasma beta value, β, increases from around 0.5 to 1.0. The electron density and temperature both increase. The ion density also increases. But ion

temperature decreases. Accompanied this dipolarization the tailward ions bulk flow, $V_{//x}$ ~ -100km/s and the perpendicular component to the magnetic field in the X direction, $V_{\perp x}$ ~ -50 km/s is detected by TH-D, as shown in Figure 3g. The perpendicular velocity in the Y direction is mainly dawnward at the beginning time of this dipolarization, $V_{\perp y}$ ~ -30km/s. The electric field detected by TH-D also has large fluctuations with negative E_y value during the first depolarization as shown in Figure 3j. During the intervals from 09:30:34 UT to 09:30:54 UT the convection electric field direction is dawnward with large magnitude, E_{cy} ~ -12 mV/m, as presented in Figure 3k. The second magnetic field elevation angle increases sharply at around 09:36 as displayed in Figure 3c marked by the right two vertical dashed lines. The elevation angle increases from about 25 degree to 45 degree during the interval from 09:36:06 UT to 09:36:21UT. The magnetic field has similar variations to the first dipolarization signatures. Especially, the second dipolarization has larger elevation angle maximum value, ~ 45 degree, as marked by the fourth vertical dashed line in Figure 3c. During the second dipolarization the tailward ions bulk flow perpendicular to the magnetic field is also detected by TH-D, $V_{\perp x}$ ~ -70 km/s, as presented in Figure 3g. Also the significant negative E_y component is companied by this intense dipolarization in Figure 3j and 3k.

Duringthe intervals of magnetic dipolarizations with tailward ions bulk flow detected by TH-D inside geosynchronous orbit, TH-E observed very weak increase in the magnetic field elevation angle and the B_z component around 09:35 UT and 09:41 UT, as shown in Figure 4b and 4c, about 5 min after two dipolarizations detected by TH-D. The ions and electrondensity andtemperature increase weakly from very low value as displayed in Figure 4d and 4e. Outside geosynchronous orbit, TH-E observed very low beta value, as shown in Figure 4f, β ~ 0.01 and β ~ 0.2 around 09:35 UT and 09:41 UT, respectively. Interesting phenomena that the weak dipolarization was with the tailward ions bulk flow, $V_{//x}$ ~ -180km/s, is also detected by TH-E around 09:35 UT as shown in Figure 4g. The perpendicular velocity is dominated in the negative Y direction, $V_{\perp y}$ ~ -50 km/s.

Associated with the intense electric field observed by TH-D inside geosynchronous orbitduring this two dipolarizations, the energy fluxes of energetic electrons, as shown in the second panel of Figure 5, with energy of 31 keV(blue), 41 keV (gray), 52 keV (red), 65.5 keV (black), 93 keV(brown) and 139 keV(purple) all simultaneously increase at 09:30:38 UT and 09:36:09UT detected by SST/TH-D, respectively. These energetic electrons have quasi-perpendicular pitch angle distribution, as presented in the bottom panel of Figure 5.

Discussion and conclusions

The dipolarizations with tailward ions bulk flow inside geosynchronous orbit are investigated in our present paper. Accompanied these dipolarizations the energy fluxes of energetic electrons with energy between 31 keV and 139 keV simultaneously increase inside geosynchronous orbit. According to these energetic electrons pitch angle distributions, it is

found that high energy electrons mainly in the quasi-perpendicular direction to the magnetic field, as shown in Figure 5. On the other hand, the inductive electric field during these two magneticdipolarization is in the dawnward direction as display in Figure 3j and 3k. Previous research work reported that the inductive electric field associated with substorm dipolarization can accelerate particles in the near-Earth plasma sheet [e.g. Dai et al., 2014, 2015; Duan et al., 2016; Fu et al., 2011; Fok et al., 2001; Liu et al., 2010; Lui et al., 1988, 1999; Nakamura et al., 2009; Nosé et al., 2014]. As shown in Figure 3j around 09:36:30 UT the inductive electric fields in the second dipolarization are dominated in the E_y component with large negative value, E_y ~ -25mV/m, and the X component also increase with negative value E_x ~ -6mV/m. This intense electric field can drive ions moving into the tailward-dawnward direction. On the other hand, we can calculate the energy quantity relationship between the electric field and energetic electrons. Estimating the energy of such intense E_y in the distance of ~1000 km is about ~ 10^{-15} Joule. The energetic electrons with energy range from 31 keV to 139 keV are in the same energy order ~10^{-15} Joule. It is inferred that the intense E_y can perpendicularly accelerate electrons to tens keV state.

Dipolarizations occurring at the inner edge of plasma sheet are complicated with disturbances of ions bulk flow and electromagnetic field. Lui et al. [1999] pointed out that near-Earth dipolarization was a non-MHD process and was also accompanied with tailward ions flow.Our observations of dipolarizations inside geosynchronous orbit are also associated with tailward ions flow. This result is consistent with the report proposed by Liu et al. [2008] that the perturbations associated with the ballooning mode in the near-Earth plasma sheet propagating tailward. Based on the statistic studies, Nosé et al. [2016] proposed that the occurrence probability of the dipolarizations in the inner magnetosphere had a peak at 21:00-00:00 MLT. Our observations show that two distinct dipolarizations with tailward flow inside geosynchronous orbit are detected by TH-D around 00:02 MLT and 00:05 MLT, respectively.

According to the distance between TH-D and TH-E, (-2.23, -2.30, 0.56)R_E, and the delay time of dipolarization from inside to outside geosynchronous orbit, ~5 min, the dipolarization propagating speed or the plasma sheet expanding speed can be estimated as V_x ~ -47 km/s, V_y ~ -48 km/s, V_z ~ 12 km/s, respectively. Liou et al. [2002] proposed that the dipolarization region expanding speed was ~ 60 km/s westward at geosynchronous. Comparing observations between TH-D and TH-E in our investigations, the azimuth speed of dipolarization region is obtained ~ 48 km/s. These two observational results are consistent with each other. The dipolarization associated with the current disruption propagated tailward with speed V_x ~ -100 km/s detected by THEMIS satellites in the near-Earth plasma sheet X~ -11R_E [Liu et al., 2008]. It is larger than the dipolarization propagating speed from inside to outside geosynchronous orbit V_x ~ -47 km/s . The different speeds of dipolarizations propagating tailward imply that the magnitude of the dipolarization speed may be associated with its beginning location in magnetotail plasma sheet.

On the other hand, Lui [1991] reported that substorm disturbance propagated tailward through a rarefaction wave front accompanied by earthward flow during substorm expansion phase early period. Chao et al. [1977] proposed that the rarefaction wave propagating tailward was accompanied by the thinning of plasma sheet and earthward plasma flow. This earthward flow is possibly convection flow or outflow flow of magnetic reconnection from the middle magnetotail.

Based on the above observation analysis, we can draw the results as following. Two distinct magnetic dipolarizations with tailward ions flow are observed by TH-D inside geosynchronous orbit on 27 August 2014 during the intense substorm with AE_{max} ~ 1000nT. TH-D was located inside geosynchronous orbit around midnight in the interval from 09:20 UT to 10:00 UT. The first dipolarization is displayed by magnetic elevation angle increase from 15 degree to 25 degree around 09:30:40UT. The second one is presented by the elevation angle increase from 25 degree to 45 degree around 09:36 UT. These two significant dipolarizations are accompanied with the energy flux of energetic electrons simultaneously increase inside geosynchronous orbit. After 5 min expanding tailward of near-Earth plasma sheet, TH-E located outside geosynchronous orbit also detects this tailward expanding plasma sheet with ion flow -150 km/s. The dipolarization propagates tailward with speed -45 km/s, along 2 R_E distant in the X direction between TH-D and TH-E within 5 min. These dipolarizations with tailward ion flow observed inside geosynchronous orbit indicate new energy transfer path in the inner magnetosphere during substorms.

Acknowledgments

We acknowledge NASA contract NAS5-02099 for use of data from the THEMIS Mission. Specifically: "D. Larson and R. P. Lin for use of SST data, C. W. Carlson and J. P. McFadden for use of ESA data; J. Bonnell and F. S. Mozer for use of the EFI data; K. H. Glassmeier, U. Auster and W. Baumjohann for the use of FGM data provided under the lead of the Technical University of Braunschweig and with financial support through the German Ministry for Economy and Technology and the German Center for Aviation and Space (DLR) under contract 50 OC 0302. The authors thank NASA CDAWeb and Taiwan AIDA for THEMIS data. The SYM − H index was provided by Data Analysis Center for Geomagnetism and Space Magnetism in Kyoto, Japan. This work is supported by the National Natural Science Foundation of China grants 41674167, 41731070 and 41574161; and in part by the Specialized Research Fund for State Key Laboratories.

References

Angelopoulos, V.: The THEMIS Mission, Space Science Reviews, 141, 5-34, 2008.

Angelopoulos, V., Baumjohann, W., Kennel, C. F., Coroniti, F. V., Kivelson, M. G., Pellat, R., Walker, R. J., Lühr, H., and Paschmann, G.: Bursty bulk flows in the inner central plasma sheet, Journal of Geophysical Research, 97, 4027, 1992.

Auster, H. U., Glassmeier, K. H., Magnes, W., Aydogar, O., Baumjohann, W., Constantinescu, D., Fischer, D., Fornacon, K. H., Georgescu, E., Harvey, P., Hillenmaier, O., Kroth, R., Ludlam, M., Narita, Y., Nakamura, R., Okrafka, K., Plaschke, F., Richter, I., Schwarzl, H., Stoll, B., Valavanoglou, A., and Wiedemann, M.: The THEMIS Fluxgate Magnetometer, Space Science Reviews, 141, 235-264, 2008.

Baumjohann, W., Hesse, M., Kokubun, S., Mukai, T., Nagai, T., and Petrukovich, A. A.: Substorm dipolarization and recovery, Journal of Geophysical Research: Space Physics, 104, 24995-25000, 1999.

Bonnell, J. W., Mozer, F. S., Delory, G. T., Hull, A. J., Ergun, R. E., Cully, C. M., Angelopoulos, V., and Harvey, P. R.: The Electric Field Instrument (EFI) for THEMIS, Space Science Reviews, 141, 303-341, 2008.

Chao J., K ., J. R . Kan, A . T. Y. Lui and S .-I. Akasofu A model for thinning of the plasma sheet, Planet. Space Sci., 25, 703-710, 1977.

Dai, L., Wang, C., Duan, S., He, Z., Wygant, J. R., Cattell, C. A., Tao, X., Su, Z., Kletzing, C., Baker, D. N., Li, X., Malaspina, D., Blake, J. B., Fennell, J., Claudepierre, S., Turner, D. L., Reeves, G. D., Funsten, H. O., Spence, H. E., Angelopoulos, V., Fruehauff, D., Chen, L., Thaller, S., Breneman, A., and Tang, X.: Near-Earth injection of MeV electrons associated with intense dipolarization electric fields: Van Allen Probes observations, Geophys Res Lett, 42, 6170-6179, 2015.

Dai, L., Wygant, J. R., Cattell, C. A., Thaller, S., Kersten, K., Breneman, A., Tang, X., Friedel, R. H., Claudepierre, S. G., and Tao, X.: Evidence for injection of relativistic electrons into the Earth's outer radiation belt via intense substorm electric fields, Geophysical Research Letters, 41, 1133-1141, 2014.

Duan, S., Liu, Z., Cao, J., Lu, L., Rème, H., Dandouras, I., and Carr, C. M.: TC-1 observation of ion high-speed flow reversal in the near-Earth plasma sheet during substorm, Science in China Series E: Technological Sciences, 51, 1721-1730, 2008.

Duan, S. P., Dai, L., Wang, C., Liang, J., Lui, A. T. Y., Chen, L. J., He, Z. H., Zhang, Y. C., and Angelopoulos, V.: Evidence of kinetic Alfven eigenmode in the near-Earth magnetotail during substorm expansion phase, Journal of Geophysical Research-Space Physics, 121, 4316-4330, 2016.

Duan, S. P., Liu, Z. X., Liang, J., Zhang, Y. C., and Chen, T.: Multiple magnetic dipolarizations observed by THEMIS during a substorm, Annales Geophysicae, 29, 331-339, 2011.

Fok, M.-C., Moore, T. E., and Spjeldvik, W. N.: Rapid enhancement of radiation belt electron fluxes due to substorm dipolarization of the geomagnetic field, Journal of Geophysical Research: Space Physics, 106, 3873-3881, 2001.

Fu, H. S., Khotyaintsev, Y. V., André, M., and Vaivads, A.: Fermi and betatron acceleration of suprathermal electrons behind dipolarization fronts, Geophysical Research Letters, 38, n/a-n/a, 2011.

Liang, J., Liu, W. W., and Donovan, E. F.: Ion temperature drop and quasi-electrostatic electric field at the current sheet boundary minutes prior to the local current disruption, Journal of Geophysical Research: Space Physics, 114, n/a-n/a, 2009.

Liou, K., Meng, C.-I., Lui, A. T. Y., Newell, P. T., and Wing, S.: Magnetic dipolarization with substorm expansion onset, Journal of Geophysical Research, 107, 2002.

Liu, W. W.: Physics of the explosive growth phase: Ballooning instability revisited, Journal of Geophysical Research: Space Physics, 102, 4927-4931, 1997.

Liu, W. W. and Liang, J.: Disruption of magnetospheric current sheet by quasi-electrostatic field in the substorm expansion phase, Annales Geophysicae, 27, 1941-1950, 2009.

Liu, W. W., Liang, J., and Donovan, E. F.: Electrostatic field and ion temperature drop in thin current sheets: A theory, Journal of Geophysical Research: Space Physics, 115, n/a-n/a, 2010.

Liu, W. W., Liang, J., and Donovan, E. F.: Interaction between kinetic ballooning perturbation and thin current sheet: Quasi-electrostatic field, local onset, and global characteristics, Geophysical Research Letters, 35, 2008.

Lui, A. T. Y., Liou, K., Nosé, M., Ohtani, S., Williams, D. J., Mukai, T., Tsuruda, K., and Kokubun, S.: Near-Earth dipolarization: Evidence for a non-MHD process, Geophysical Research Letters, 26, 2905-2908, 1999.

Lui, A. T. Y., Lopez, R. E., Krimigis, S. M., McEntire, R. W., Zanetti, L. J., and Potemra, T. A.: A case study of magnetotail current sheet disruption and diversion, Geophysical Research Letters, 15, 721-724, 1988.

Lui, A. T. Y., A synthesis of magnetospheric substorm models, Journal of Geophysical Research, 96,1849, 1991.

McFadden, J. P., Carlson, C. W., Larson, D., Ludlam, M., Abiad, R., Elliott, B., Turin, P., Marckwordt, M., and Angelopoulos, V.: The THEMIS ESA Plasma Instrument and In-flight Calibration, Space Science Reviews, 141, 277-302, 2008.

Miyashita, Y., Machida, S., Mukai, T., Saito, Y., Tsuruda, K., Hayakawa, H., and Sutcliffe, P. R.: A statistical study of variations in the near and middistant magnetotail associated with substorm onsets: GEOTAIL observations, Journal of Geophysical Research: Space Physics, 105, 15913-15930, 2000.

Nagai, T.: Observed magnetic substorm signatures at synchronous altitude, Journal of Geophysical Research, 87, 4405, 1982.

Nakamura, R., Retino, A., Baumjohann, W., Volwerk, M., Erkaev, N., Klecker, B., Lucek, E. A., Dandouras, I., Andre, M., and Khotyaintsev, Y.: Evolution of dipolarization in the near-Earth current sheet induced by Earthward rapid flux transport, Annales Geophysicae, 27, 1743-1754, 2009.

Nosé, M., Keika, K., Kletzing, C. A., Spence, H. E., Smith, C. W., MacDowall, R. J., Reeves, G. D., Larsen, B. A., and Mitchell, D. G.: Van Allen Probes observations of magnetic field dipolarization and its associated O+ flux variations in the inner magnetosphere at L < 6.6, Journal of Geophysical Research-Space Physics, 121, 7572-7589, 2016.

Nosé, M., Takahashi, K., Keika, K., Kistler, L. M., Koga, K., Koshiishi, H., Matsumoto, H., Shoji, M., Miyashita, Y., and Nomura, R.: Magnetic fluctuations embedded in dipolarization inside geosynchronous orbit and their associated selective acceleration of O+ ions, Journal of Geophysical Research: Space Physics, 119, 4639-4655, 2014.

Ohtani, S., Motoba, T., Gkioulidou, M., Takahashi, K., and Singer, H. J.: Spatial Development of the Dipolarization Region in the Inner Magnetosphere, Journal of Geophysical Research: Space Physics, 123, 5452-5463, 2018.

Saito, M. H., Miyashita, Y., Fujimoto, M., Shinohara, I., Saito, Y., Liou, K., and Mukai, T.: Ballooning mode waves prior to substorm-associated dipolarizations: Geotail observations, Geophysical Research Letters, 35, n/a-n/a, 2008.

Shiokawa, K., Baumjohann, W., Haerendel, G., Paschmann, G., Fennell, J. F., Friis-Christensen, E., Lühr, H., Reeves, G. D., Russell, C. T., Sutcliffe, P. R., and Takahashi, K.: High-speed ion flow, substorm current wedge, and multiple Pi 2 pulsations, Journal of Geophysical Research: Space Physics, 103, 4491-4507, 1998.

Figure 1 The solar wind, IMF $\boldsymbol{B_z}$ conditions and geomagnetic indices between 01:00 UT and 23:00 UT on August 27, 2014. From top to bottom of (a ~ g) panels show the change of solar wind dynamic pressure (a), $\boldsymbol{B_{z,IMF}}$ in GSM coordinate (b), the x component of the solar wind flow speedin GSM coordinate (c), electric field$\boldsymbol{E}$ (d), *AE/AU/AL* index (e),*SYM-H* indices (f), and *ASY-H* index (g). From left to right, the verticaldotted lines in (a ~ g) panels marked the time 01:48 UT, 06:42 UT, 09:31 UT, 09:48 UT, 21:56 UT and 22:35 UT, respectively.

Figure 2 The orbits of TH-D and TH-E in the $\boldsymbol{X-Y_{SM}}$ plane and the $\boldsymbol{X-Z_{SM}}$ plane from 09:20 to 10:00 UT on 27 August 2014, which were in the nightside magnetosphere. The arrow shows the flying direction of the satellites. TH-D is redand TH-E is blue.

Figure 3 The electromagnetic field and plasma parameters detected by TH-D in the intervals from 09:25 UT to 09:55 UT on August 27, 2014. The Solar Magnetic (SM)coordinated system is adopted. From top to bottom, panels showed that (a)the total magnetic field $\boldsymbol{B_t}$ (black) and the X component $\boldsymbol{B_x}$ (red), (b) the Y component $\boldsymbol{B_y}$ (green) and the Z component $\boldsymbol{B_z}$ (blue), (c)the magnetic field elevation angle $\boldsymbol{\theta}$; (d) ion and electron density $\boldsymbol{N_i}$, $\boldsymbol{N_e}$; (e)ion and electron temperature $\boldsymbol{T_i}$, $\boldsymbol{T_e}$; (f) plasma beta $\boldsymbol{\beta}$; (g) the X component of ion parallelvelocity and perpendicular velocity $\boldsymbol{V_{parx}}$, $\boldsymbol{V_{perpx}}$; (h) the Y component of ion parallel velocity and perpendicularvelocity $\boldsymbol{V_{pary}}$,$\boldsymbol{V_{perpy}}$; (i) the Z component of ion parallel velocity and perpendicular velocity $\boldsymbol{V_{parz}}$, $\boldsymbol{V_{perpz}}$; (j) the electric field $\boldsymbol{E_x}$ (red), $\boldsymbol{E_y}$ (black), and $\boldsymbol{E_z}$ (blue) by assuming $\mathbf{E}\cdot\mathbf{B}=\mathbf{0}$; (k) the electric field $\boldsymbol{E_{cx}}$ (red), $\boldsymbol{E_{cy}}$ (black), $\boldsymbol{E_{cz}}$ (blue) calculated by $\mathbf{E}=\mathbf{B}\times\mathbf{V}$. The black vertical dashed lines marked the time 09:30:34 UT,09:30:54UT, 09:36:06 UT and 09:36:21 UT, respectively.

Figure 4 The electromagnetic field and plasma parameters detected by TH-E in the intervals from 09:25 UT to 09:55 UT on August 27, 2014.The Figure format is the same as Figure 3.The black vertical dashed lines marked the time 09:35:36 UT and 09:36:18 UT.

Figure 5 The energy flux and pitch angle distribution of energetic electrons detected by SST/TH-D in 3 second time resolution. The red vertical lines marked the time 09:30:38 UT and 09:36:09 UT.

Figure 1

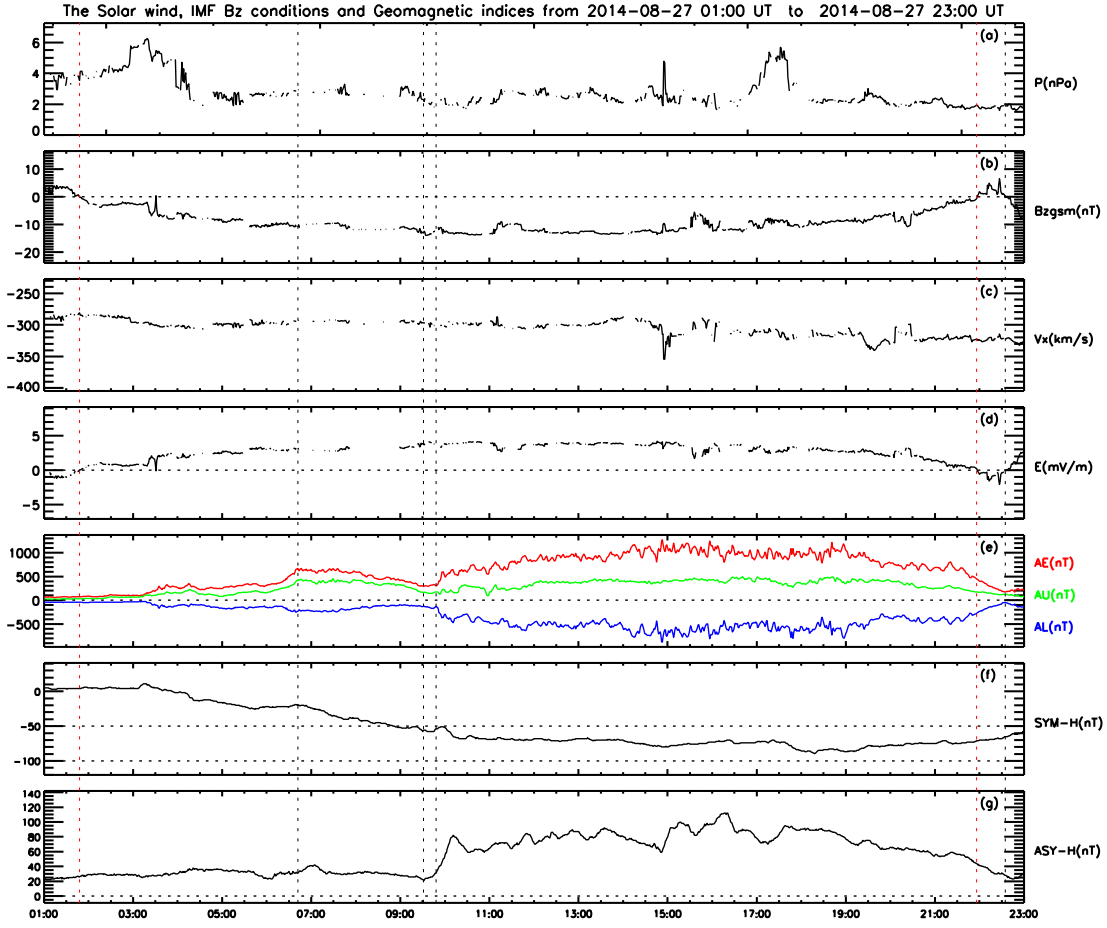

Figure 2

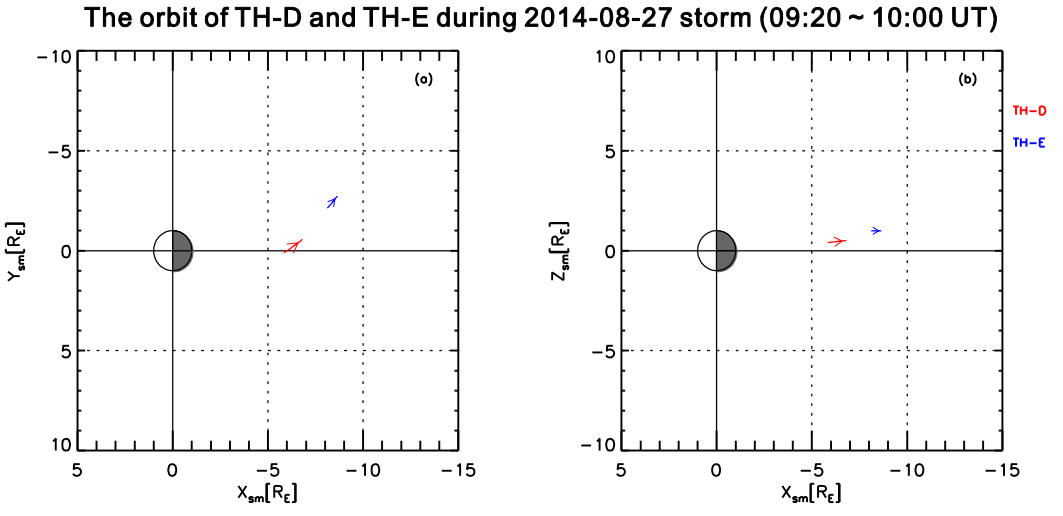

283 Figure 3

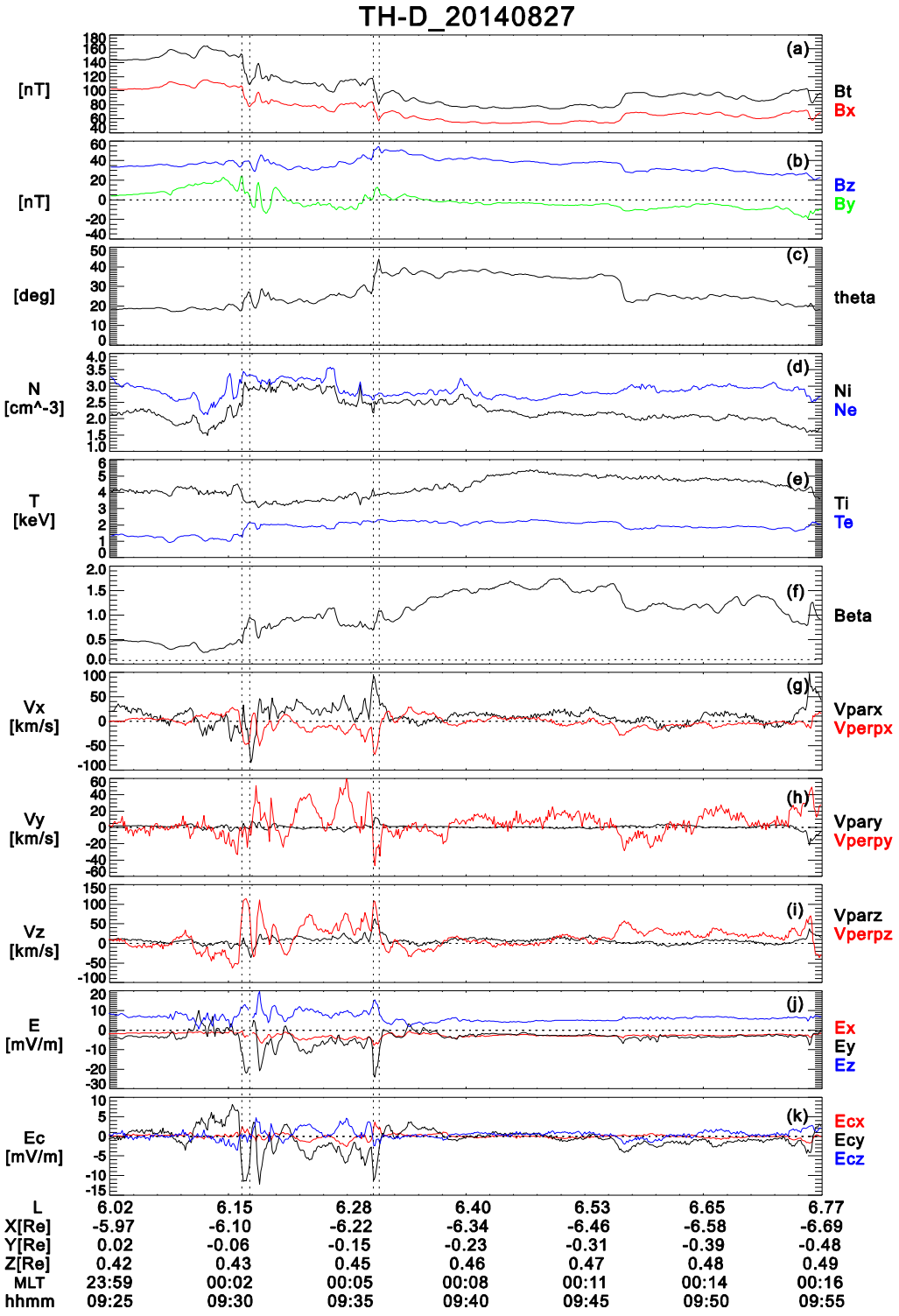

284

285 Figure 4

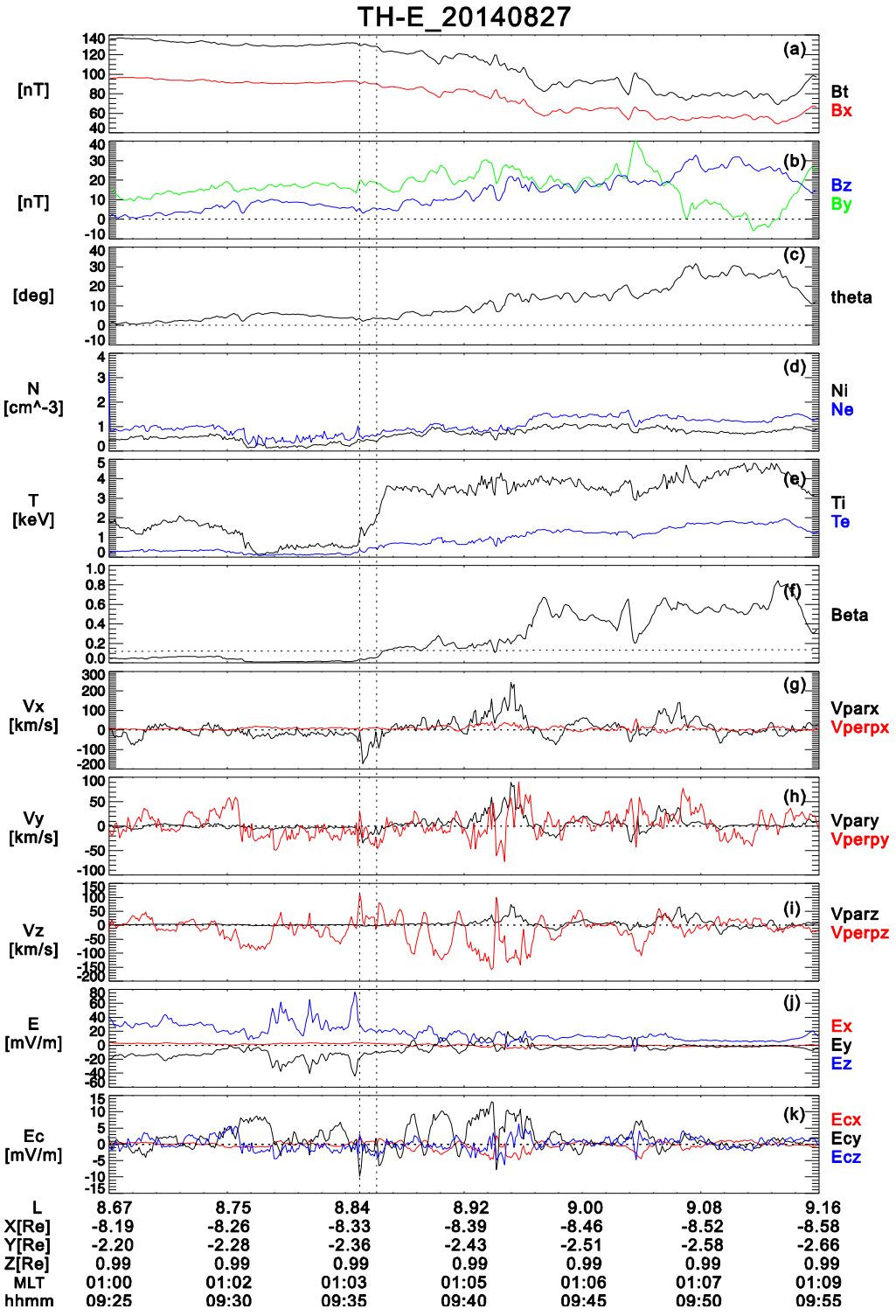

286

287 Figure 5

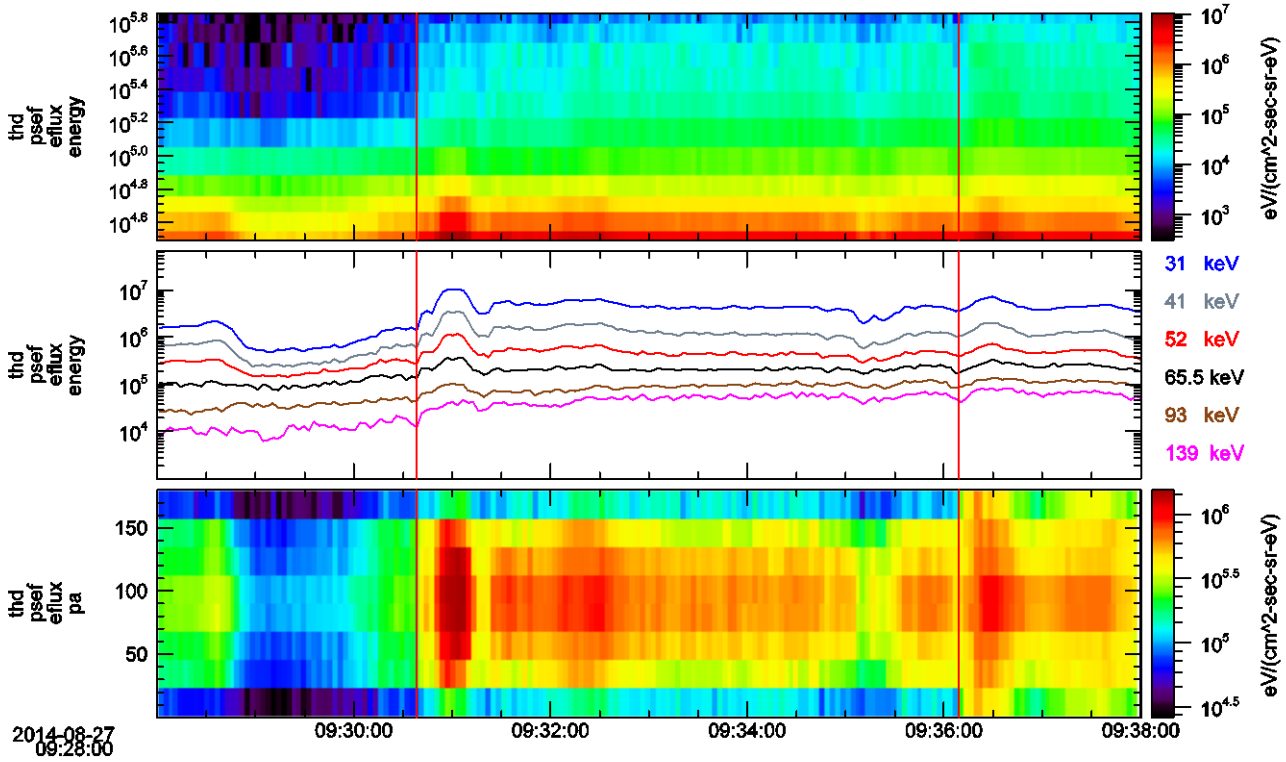

288

289